Robust H∞ optimal controller designs for feedback substitution schemes using LSDP and MOGA 9th IEEE International Conference in Systems Man and Cybernetics

Robust H^{∞} Optimal Controller Designs for Feedback Substitution Schemes using LSDP and MOGA

Mirsha M. Trujillo
Cybernetics, School of Systems Engineering, The University of Reading RG6 6AY, UK
vj014789@student.reading.ac.uk

Sillas Hadjiloucas
Cybernetics, School of Systems Engineering, The University of Reading RG6 6AY, UK
s.hadjiloucas@reading.ac.uk

Victor M. Becerra
Cybernetics, School of Systems Engineering, The University of Reading RG6 6AY, UK
v.m.becerra@reading.ac.uk

Abstract—**We discuss a new methodology for designing optimal controllers tailored specifically for feedback substitution schemes. The loop shaping design procedure (LSDP) requires us to re-cast the problem using linear matrix inequalities to specify a range of objectives. We then use a genetic algorithm to perform a multi-objective optimization for the controller weights (MOGA). We contrast this methodology to that currently adopted to simultaneously minimize response time and noise variance in the feedback signal in simple SISO systems. We use robust control theory criteria to benchmark the performance of the designed controllers and compare them to those derived using analytical techniques.**

Keywords-optimal control, robust control, multi-objective optimization; genetic algorithms.

I. INTRODUCTION

Feedback substitution schemes relate to a special class of feedback systems. They arise when a feedback system designed to track a physical process is replaced by another one, which has identical dynamics but takes place in another transduction domain. A requirement is that the process in the new transduction domain, once re-converted to the original domain, must have an overall effect that nulls the disturbance.

One can find many examples of feedback substitution schemes, mostly in biology (e.g., homeostasis, hormonal control etc). An important characteristic of feedback substitution schemes is that there are contradicting objectives that must be simultaneously fulfilled. The first objective is to ensure the maximum gain-bandwidth product possible, this relates to achieving a minimum response time. The second is an accurate estimation of the external disturbance. It is clear that the variance in the noise related to the measurement of this disturbance can only be minimized by increasing the measurement time.

For simple systems, analytical techniques have been developed that lead to optimal controller designs that minimize the variance in the noise while at the same time the response time of the loop is kept to a minimum [1]. The technique, however, is restricted to low order controllers. The purpose of this work is to provide an alternative methodology that allows the design of higher order controllers. Anticipated advantages of using higher order controllers are a better response time for the same amount of variance in the noise and a better robustness of the loop. The proposed methodology is also more generic and will permit the design of controllers after taking into considerations additional requirements that might have to be simultaneously satisfied. For brevity, we confine our analysis to single input single output (SISO) systems.

The problem specifications indicate this is a goal attainment problem, which may be translated to a multi-objective minimization formulation. The optimization problem is cast as a set of n design objective functions $\phi_i(\mathbf{p}) : i = 1...n$ where $\mathbf{p}$ denotes the design parameters $\mathbf{p} = (p_1, p_1 \ldots p_n)$ chosen and our task is to find: $\min_{p \in P} \{\phi_i(\mathbf{p}), \text{for } i = 1...n\}$, where P denotes the entire set of possible design parameters (in the simplest form of the problem $i = 2$).

As stated earlier, the design parameters are in conflict so the result of the multi-objective optimization is a Pareto-optimal solution. This inter-relation between the solutions, implies that for a point $\mathbf{p}^* \in P$, there exists no other point such that $\phi_i(\mathbf{p}) \le \phi_i(\mathbf{p}^*) \forall\, i = 1...n \wedge \phi_j(\mathbf{p}) < \phi_j(\mathbf{p}^*)$ for at least one j.

Because there can be a large set of Pareto-optimal solutions to choose from, the design problem is re-formulated using the method of inequalities (MOI). We can impose a set of inequalities in the time or frequency domain which need to be simultaneously satisfied: $\phi_i(\mathbf{p}) \le \varepsilon_i$ for $i = 1...n$ where $\varepsilon_i \in \mathbb{R}^q \subseteq \mathbb{R}^n$. Our aim is to find a vector $\mathbf{p}$ of admissible points that simultaneously satisfy all the inequalities.

In previous works adopting the method of inequalities [2], the functions $\phi_i(\mathbf{p})$ where functionals of the system step response, e.g., rise-time, overshoot, integral absolute error or of frequency response such as the bandwidth. They may also represent measures of the system stability and robustness, such as the maximum real part of the closed-loop poles. Alternatively, $\mathbf{p}$ may parameterize the weighting functions required by analytical optimization methods to provide a mixed optimization approach. To our knowledge, however, this is the first time that a measure of the internal noise in the transduction process is explicitly incorporated in the design parameters for minimization.

There are many ways one can find an admissible point in conflicting requirements of a Pareto-optimization. The moving boundaries process (MBP) [2] uses Rosenbrock's hill-climbing routine [3] to perform a local search to improve on at least one of the unsatisfied performance indices. The results of the MBP

process, however, are sensitive to the starting point. The Nelder Mead Dynamic Minimax method (NMDM) [4] is an alternative method but it has been suggested that it is also sensitive to the starting point [2]. In this work, we have used a multi-objective genetic algorithm (MOGA) as developed by Fonseca and Fleming [5] to seek several simultaneous Pareto-optimal or near Pareto-optimal solutions and we then select the best solution from the set. The MOGA is set into a multi-objective context by means of a fitness function. The individuals are ranked on the basis of the number of other individuals and are then assigned a fitness value according to their rank.

A normalized co-prime factorization of the shaped plant is introduced [6,7] to model transducer internal noise and external perturbations as uncertainties to the co-prime factors of the shaped plant. A mixed optimization approach is adopted where the MOI is used to also design the weighting functions (a pre-compensator and a post-compensator) of a Loop Shaping Design Procedure (LSDP) [6]. LSDP is used to design an open loop function that meets all the requirements and then an H^{∞} controller is synthesized to robustly stabilize the closed loop. An advantage of LSDP is that it maximizes robust stability to perturbations. MOGA is employed to get the optimal weighting functions in the LSDP formulation of the problem.

In order to establish the proposed controller design methodology as an alternative for controller design in feedback substitution schemes, we first need to benchmark it to performance metrics related to the analytical expressions of a SISO system. A 1st order system followed by a 1st order low-pass filter for which well established analytical techniques have been used to derive 2nd order optimal controllers is considered. In the following sections, we elaborate on the different aspects that relate to the individual elements of the methodology adopted.

II. Optimal Controler Design in a Simple Feedback Substitution Scheme Using Analytical Techniques

In its simplest form, a Feedback Substitution Scheme (FSS) comprises a transducer, followed by a filter and controller as well as a second transducer as illustrated in Fig. 1. $W_r(s)$ is the external signal to be nulled through the first transduction process, $G(s)$ is the transfer function of the transducer that measures the external input, $F(s)$ represents a low pass filter, $K(s)$ is the controller to be designed and $W_f(s)$ is the action of the second transducer, given a controller response, aiming to oppose the effect of $W_r(s)$ in the first transduction process $\left(W_f(s) = -W_r(s)\right)$. The output $W_f(s)$ is the combination of the input and noise transfer functions. For simplicity, we assume that the dynamics of the 2nd transduction process power are very fast, compared to the other processes in the system, so that its transfer function amounts to a gain g.

In Fig. 2a, we represent a modulated external disturbance W_r of arbitrary order to the system. The feedback signal W_f (Fig. 2b) is generated to counteract the external input. This signal incorporates the low-pass characteristics of the detection process as well as the dynamics of the controller. The entire system operates within certain specifications in terms of response time and overshoot. The detector output produces a signal in response to the reference V_a which provides always a reference d.c. offset despite external perturbations (Fig. 2c).

The main objective in this system is to optimize the two conflicting requirements; Response time t_r and noise power gain G. The response time t_r is defined as the time required for the system to produce a signal $W_f = -(W_r - \varepsilon_T)$ where $\pm\varepsilon_T$ is a tolerance level. After time t_r, $W_f = W_r \pm \varepsilon_T$.

The observed variance in the output is mainly due to fluctuations introduced by the transducer itself (self-noise). These fluctuations can be represented by a noise signal $u_d(s)$ introduced to the system at the output of the transducer. The response of the system to $u_d(s)$ is the transfer function $Q(s)$ from V_d to W_f. Following the work from Clare and White [1], the total variance in the output is given by

$$\sigma^2 = \frac{1}{\tau}\left(\frac{u_d}{\Re}\right)^2 \frac{\tau}{4\pi j}\int_{-\infty}^{\infty} |Q(s)|^2\, ds\Big|_{s=j\omega} = \frac{1}{\tau}\left(\frac{u_d}{\Re}\right)^2 \mathsf{G}^2 \qquad (1)$$

where $\Re$ is the gain of the transducer and G is the noise power gain of the system. For a third order system, an expression for G is derived [8] using the method of residues [9].

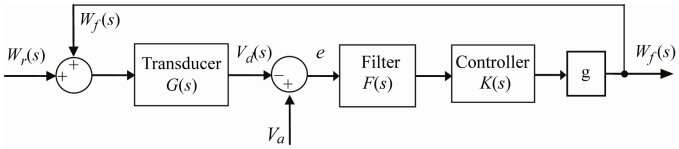

Figure 1. Block diagram of a typical Feedback Substitution Scheme.

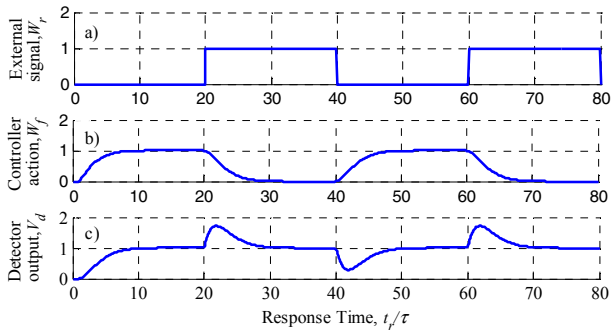

Figure 2. Response and behaviour of a feedback substitution system to an external input W_r in a), The controller action W_f in b). and the output of the detector V_d in c).

If the noise transfer function is given from:

$$Q(s) = \frac{1 + c_1 s + c_2 s^2}{1 + b_1 s + b_2 s^2 + b_3 s^3} \qquad (2)$$

the corresponding noise power gain G is:

$$\mathsf{G} = \sqrt{\frac{c_2^2 b_1 + b_3(c_1^2 - 2c_2) + b_2 b_3}{4 b_3 (b_1 b_2 - b_3)}} \qquad (3)$$

This expression describes the noise power related to third order systems only, and more complicated expressions need to be adopted for higher order systems [9]. In section III a different technique is introduced to deal with higher order systems obtained with the H^{∞} synthesis. The noise power gain G is a good performance index of how the system responds to noise, thus, this is taken as one of the objectives to minimize.

In the simplest implementation of the system, the transfer function of the transducer is of first order system with time constant τ . This is a part of the system that may not be changed. The filter $F(s)$ and the controller $K(s)$ have transfer functions that can be changed accordingly to obtain the desired response. In its simplest form, the filter has a low pass response of first order, with time constant τ_f and gain μ_f . The controller is a PI controller with gain μ_i and integration time constant τ_i. The optimization parameters are an overall gain of the system as a single parameter $\mu = \mu_d \mu_f \mu_i$, a normalized time constant of the filter with respect to τ denoted as x and a normalized integration time constant of the controller, y . The tolerance for the output overshoot is set to $\varepsilon_T = 0.001$. The two design parameters μ and x are varied in the range 0.01 to 10 and then the parameter y is adjusted to obtain the desired overshoot for each combination of μ and x. The range of μ and x values form the axes of the contour graph in Figs. 3 and 4 and plots of noise power gain G and normalized response time t_r / τ are obtained.

All of the systems described in Figs. 3 and 4 are optimal. The isoclines denote the domain of possible solutions. The most practical optimal system, however, is the one when the filter time constant is equal to the time constant of the transducer and the system response is reduced from third order to second order.

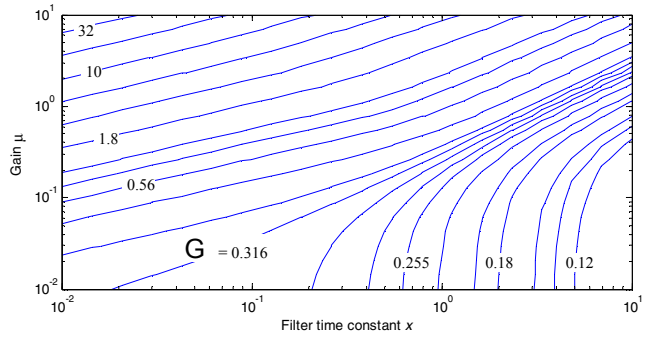

Figure 3. Contours of noise power gain G for different filter time constants x and overall loop gain μ .

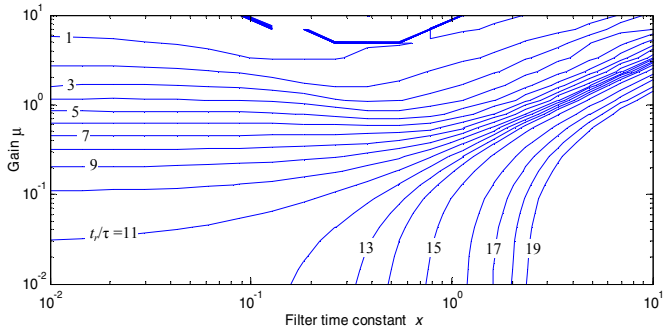

Figure 4. Contours of normalized response time t_r / τ for different filter time constants x and overall loop gain μ .

III. Loop Shaping Design Procedure with H∞ Synthesis and GAs

A. *Loop shaping and co-prime factorization*

The system described in section II can be casted to a Loop Shaping Design Procedure (LSDP) and an H-infinity controller can be synthesized as described by McFarlane and Glover [6]. The design parameters μ, x, and y are substituted by weighting functions W_1 and W_2 to shape the plant G to achieve the desired response. The H-infinity controller is synthesized to robustly stabilize the closed loop system. The shaped plant G_s is shown in Fig. 5a

A normalized co-prime factorization of the shaped plant $G_s = NM^{-1}$ satisfying $MV + NU = 1$ is used to model uncertainty as perturbations Δ_N and Δ_M to the co-prime factors of the shaped plant resulting in a perturbed plant G_Δ as shown in Fig. 5b.

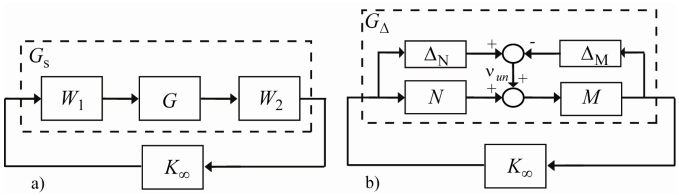

Figure 5. LSDP formulation and co-prime factorization of the system.

The perturbations Δ_N and Δ_M are stable transfer functions with uncertain dynamics and parameters, the only thing known about this transfer functions is that their H^∞ norm is less than a value ε_{sm} which is interpreted as the stability margin of the system. The resulting perturbed plant equation is:

$$G_\Delta = \left\{ (M + \Delta_M)^{-1} (N + \Delta_N) : \left\| \begin{bmatrix} \Delta_N & \Delta_M \end{bmatrix} \right\|_\infty < \varepsilon_{sm} \right\} \quad (4)$$

To maximize the stability margin ε_{sm} , a controller is calculated to minimize the function

$$\gamma := \left\| \begin{bmatrix} K(1-KG)^{-1} M^{-1} \\ (1-KG)^{-1} M^{-1} \end{bmatrix} \right\|_\infty \leq \frac{1}{\varepsilon_{sm}} \quad (5)$$

where γ is the H_∞ norm of the system in Fig. 6 from v_{un} to $\begin{bmatrix} u & y \end{bmatrix}^T$ and $(1-KG)^{-1}$ is the sensitivity function S . As described in [6] the maximum stability margin ε^*_{sm} value achievable is given by the equation

$$\varepsilon^*_{sm} = \left\{ 1 - \left\| \begin{bmatrix} N & M \end{bmatrix} \right\|_H^2 \right\}^{-\frac{1}{2}} \quad (6)$$

with $\|\bullet\|_H$ denoting the Hankel norm.

To solve (5) we formulate the plant in standard state space form:

$$G(s) = D + C(sI - A)^{-1} B \overset{s}{=} \left[\begin{array}{c|c} A & B \\ \hline C & D \end{array} \right] \quad (7a)$$

where:

$$\begin{bmatrix} N & M \end{bmatrix} \overset{s}{=} \left[\begin{array}{c|cc} A + HC & B + HD & H \\ \hline R^{-1/2} C & R^{-1/2} D & R^{-1/2} \end{array} \right] \quad (7b)$$

is a normalized co-prime factorization of G, with $H=-\left(BD^T+ZC^T\right)R^{-1}$, $R=I+DD^T$ and use the two Riccati equations, with unknowns Z and X:

$$\left(A-BS^{-1}D^TC\right)Z+Z\left(A-BS^{-1}D^TC\right)^T-ZC^TR^{-1}CZ+BS^{-1}B^T=0 \quad (8a)$$

$$\left(A-BS^{-1}D^TC\right)^TX+X\left(A-BS^{-1}D^TC\right)-XBS^{-1}B^TX+C^TR^{-1}C=0 \quad (8b)$$

where $S=I+D^TD$. The controller is given from:

$$K:=\left[\begin{array}{c|c}A+BF+\gamma^2\left(L^T\right)^{-1}ZC^T\left(C+DF\right) & \gamma^2\left(L^T\right)^{-1}ZC^T\\ \hline B^TX & -D^T\end{array}\right] \quad (9)$$

where $F=-S^{-1}\left(D^TC+B^TX\right)$, $L=\left(1-\gamma^2\right)I+XZ$.

As discussed in [6], we move the pre- and post-compensator weights from the plant in Fig. 5 to the controller $W_2K_\infty W_1$.

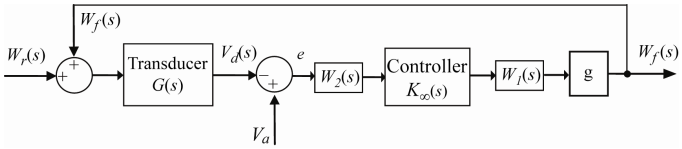

Figure 6. LSDP formulation of the feedback substitution scheme.

In the following section, the procedure to obtain the weighting functions is described.

B. Optimal design of weighting functions

Because of the precision of the system's overshoot requirement, a systematic and iterative strategy is needed to design the weighting functions W_1, W_2. A procedure that has been used in different applications [10, 11] is described in this section.

First the system requirements are specified using a representation similar to that used in the method of inequalities. These inequalities define a goal attainment problem which is translated into a minimization problem. A Multi-objective Optimization with Genetic Algorithms (MOGA) from MATLAB's Genetic Algorithm and Direct Search toolbox V2.4.1 (R2009a) the function '*gamultiobj*' is used to find the parameters and structure of the weighting functions that lead to an optimum solution.

The design requirements for the system are as follows: The output $W_f(t)$ for a unitary step input $W_r(t)=1$ must have an overshoot $\varepsilon_T=0.001$ which is specified to a numerical precision of $\varepsilon_T/500$; after the first overshoot, the output $W_f(t)$ must remain within the range $1\pm\varepsilon_T$; the noise power gain G in the newly designed system must be minimized for all normalized response times considered. Additional requirements are a zero steady state and a robust stability margin ε_{sm} >0.25. Systems with a normalized response time t_r/τ in the range 1 to 20 are only considered.

Using inequalities, the above specifications are casted as follows:

$$\varphi_1=\left|W_h\left[t,W_r(t)\right]-\frac{\varepsilon_T}{500}\right|\le W_r(t)+\varepsilon_T,\quad t>0 \quad (10a)$$

$$\varphi_2=\left|W_h\left[t,W_r(t)\right]-\frac{\varepsilon_T}{500}\right|\le W_r(t)-\varepsilon_T,\quad t>t_r \quad (10b)$$

$$\varphi_3=\min\sqrt{\frac{\tau}{4\pi j}\int_{-\infty}^{\infty}\left|Q(s)\right|^2\,ds}\,\Big|_{s=j\omega} \quad (10c)$$

$$\phi_4=\left\|\begin{bmatrix}K(1-KG)^{-1}M^{-1}\\(1-KG)^{-1}M^{-1}\end{bmatrix}\right\|_\infty\le\frac{1}{0.25} \quad (10d)$$

A vector of designer objective functions $\Phi=\left[\varphi_1\ \ \ldots\ \ \varphi_4\right]^T$ with p_j design parameters and objectives ε_i each, with $\varphi_i\left(p_j\right)\le\varepsilon_i$ is constructed with an admissible set composed of all admissible points.

The minimization problem is then solved using a MOGA. An auxiliary vector $\boldsymbol{\lambda}$ is required to translate the goal attainment problem into a minimization MOGA problem. Each element of the vector is given by:

$$\lambda_i\left(p_j,\varepsilon_i\right)=\begin{cases}0 & \text{if}\quad \varphi_i\left(p_j\right)\le\varepsilon_i\\ \varphi_i\left(p_j\right)-\varepsilon_i & \text{if}\quad \varphi_i\left(p_j\right)>\varepsilon_i\end{cases} \quad (11)$$

The purpose of this auxiliary vector is to provide the MOGA with a vector of fitness functions where the fitness value is a minimum (zero) if the goal is attained. The difference between the actual value and the goal is returned if the goal is not attained.

We assume the weighting function W_1 to be composed of several lead-lag structures of first or second order. This approach ensures that we can have complex poles and zeros. The coefficients for the lead-lag structures are provided from the design parameters p_j. In order to explore different parameters as well as different structures with the same MOGA with the purpose of finding optimum solutions, the MOGA has to work in a hierarchical structure as proposed in [12]. Here the parameter vector p_j is divided into two different chromosomes (Fig. 7). One chromosome corresponds to the coefficients of the weighting function. The other one controls the activation or suppression of elements in the lead-lag structure.

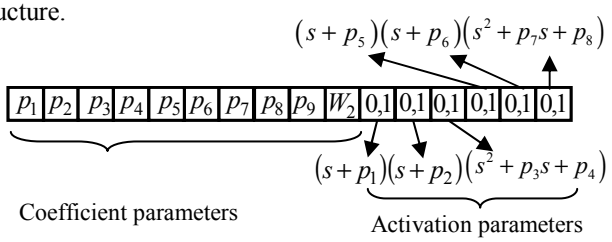

Figure 7. Chromosome separation for hierarchical GA.

The activation parameters p_{11-16}, $p_j\in\left[0\ \ 1\right]$ change the structure of the lead-lag filters in W_1, whereas the filter coefficients are given from p_{1-9}, $p_j\in\mathbb{R}$. The weighting function W_2 is assumed to have a structure of a simple gain given from p_{10}. In addition, we are including one more integrator with a very small value $(s+\upsilon)^{-1}$ (with $\upsilon=10^{-6}$) to

avoid poles in the origin that lead to internal instability when the controller is synthesized. W_1 is calculated from:

$$W_1 = p_9\left[\frac{(s+p_5)(s+p_6)(s^2+p_7 s+p_8)}{(s+\upsilon)(s+p_1)(s+p_2)(s^2+p_3 s+p_4)}\right] \qquad (12)$$

Each parameter that forms part of W_1 and W_2 in the MOGA is initially randomly initiated. For each individual in the population, the procedure in section IIIa is followed to synthesize a controller for the system as shown in Fig. 7. That system is simulated using a step response so that from the simulation, the objectives (response time, overshoot and noise power gain) can be measured. Then the MOGA uses these objectives as fitness functions to rank the produced solution according to how close they are to the Pareto-optimal front. The fittest solutions are selected for recombination and mutation. The stopping criterion is based on meeting the overshoot objective while at the same time minimizing the noise power gain. Instead of finding directly the minimum normalized response time, our strategy was to minimize the noise over small bands (± 0.15) of set values of response time.

The GA mapped the surface of all possible H^∞ controllers that can be designed with the specifications provided in the MOI. The proposed methodology permits us to analyze designed plants of up to 7th order assuming an open structure.

IV. RESULTS

A. *MOGA convergence satisfying the overshoot objective*

Simulations were initialized with a population size of 30, (type: Double Vector for coefficient parameters and Bit String for activation parameters). Although, normally, the default Pareto front population fraction is 0.35, this was changed to 0.7 to speed-up the solution. The stopping criterion for the simulations was enforced either when the overshoot objective was met or after 30 consecutive generations lapsed without an improvement in the objective functions beyond the precision default value set (10^{-6}). At each generation, a tournament selection method of size 2 was adopted (a pair-wise selection across all 30 individuals in the population). The number of individuals selected for mating (passed to the crossover function) was set to 80% of the total and a constraint dependent mutation function was adopted. Since the '*gamultiobj*' function only accepts one type of values for the population (double vector or bit string values) additional steps where incorporated to the default MATLAB functions for creation, mutation and crossover to manage the two chromosome hierarchical structure. These steps involved normalization and rounding of each activation parameter to convert them into a Bit String value.

The Pareto-optimal front has a 3-D topology. For each run of the MOGA algorithm, the overshoot objective is defined as a single valued function. The other two objectives (noise power gain and response time) form a Pareto-front. Only the solutions satisfying the first objective are kept in the simulations. Fig. 8a shows the diversity of the GA population at an early stage whereas Fig. 8b shows the convergence of the population to a solution that satisfies the overshoot objective.

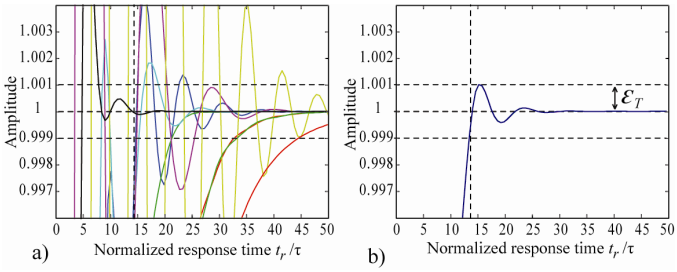

Figure 8. Step response of different individuals in the MOGA population at a) an early stage and b) a final stage of the convergence.

B. *Comparison of the analytical solution to the H^∞ solution*

Figure 9 shows a comparison of the step response obtained using the analytical approach (dashed line) discussed in Section II which is contrasted to that obtained using the H-infinity with MOGA approach (solid line).

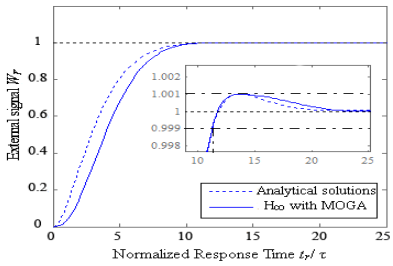

Figure 9. Step response of both systems obtained using the analytical approach (dashed line) and using the MOGA approach (solid line).

Figures 10a and 10b depict a Bode plots of the complementary sensitivity T and sensitivity S obtained using the analytical approach (dashed line) and the MOGA approach (solid line). A faster roll-off is observed for the higher order system. The corresponding phases are shown in Figs. 10c-d.

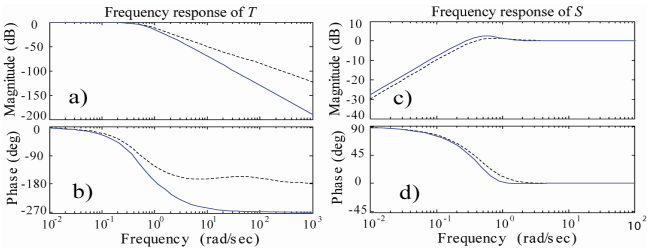

Figure 10. Bode plots of sensitivity and complementary sensitivity functions for systems with derived controllers using the analytical approach (dashed line) and the MOGA approach (solid line).

C. *Comparison of Response time and Noise Power gain*

Contours from Fig. 3 and 4 can be plotted in a single graph that represents all the possible systems resulting from the combination of design parameters used in section II. Fig. 11 shows the compromise between response time and noise power gain G for all systems fulfilling the overshoot requirement. It resembles a Pareto-optimal front which is used as a reference to compare with the optimal solutions achievable with the LSDP and H^∞-MOGA controller design process. The circles below the reference plot are the solutions found after adopting the methodology described in section III. We can see that a new notional Pareto-front dominating the previous ones is generated by the MOGA. This is so because the strategy used in section II limits the achievable time-domain response by limiting the order of the system. The higher order controller

designed through the H$^\infty$-MOGA process can provide lower noise power gain for the same normalized response time.

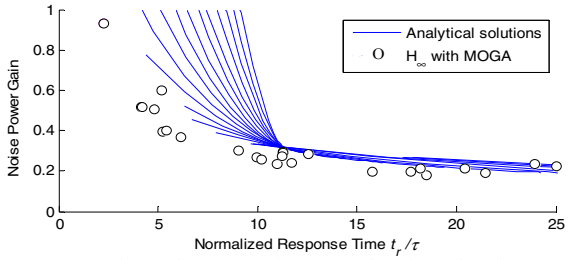

Figure 11. Comparison of response times as a function of noise power gain G using the analytical solutions approach to design the controller and the H$^\infty$-MOGA procedure.

D. Robustness analysis for the two systems.

The robust stability of the systems designed with the two procedures (analytical solution and H$^\infty$-MOGA) is assessed by means of the normalized co-prime stability margin ε_{sm} obtained through (5). Once the controller is designed using the analytical technique, the plant and controller are re-arranged in the standard form shown in Fig. 5b and the stability margin is calculated. This is compared to that obtained directly through the H$^\infty$-loop shaping procedure where the controller was designed using the MOGA. This stability margin ε_{sm} is plotted against the normalized response time in Fig. 12.

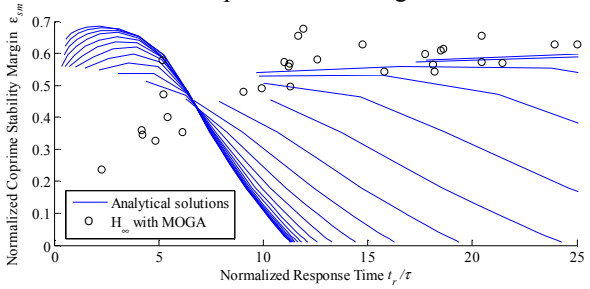

Figure 12. Normalized response time as a functin of co-prime stability margin

In the current study, the robustness design objective φ_4 was limited to a value of 4 or less.

V. DISCUSSION

The current MOGA scheme has a starting point of meeting a stability margin of 0.25. Unfortunately, it cannot find easily solutions that have the exact overshoot characteristics while satisfying the other two constrains. If we were to relax the overshoot constrain and convert this into a range, a 3D Pareto-optimal front can be found, but then the comparison of the two methodologies would not be valid. By minimizing the overshoot, we could have another range of possible solutions. Many systems can easily be found, that do not have any overshoot but satisfy the other two objectives. The precision of the overshoot constraint present in this problem adds extra difficulty to the GA to find optimal and feasible solutions; hence, sophisticated constraint handling techniques are needed. By defining the overshoot as an objective in the MOGA and not as a constraint, three different solutions are found, these minimize one objective at a time.

VI. CONCLUSION

Optimal feedback substitution schemes having a controller of first or second order can be analytically found satisfying precise overshoot characteristics, while at the same time minimizing response time and noise power gain. The design of higher-order controllers is possible using LSDP and an H$^\infty$-MOGA procedure. In this work we have handled constrains using MOGA converting them into objectives. Because the MOGA has a very limited domain of feasible solutions, we plan to use particle swarm optimization combined with GAs in the future. This is so, because the derived MOGA population often is outside the feasible solution space and another constrain handling algorithm needs to be used to move this population within the feasible solutions space. The current work shows that there is a need to adopt alternative computational intelligence algorithms that will tune the parameters of higher order systems. Future work will, therefore, concentrate on the development of artificial immune systems algorithms for the particular problem as they have shown potential for improved convergence. We also intend to combine subspace systems identification procedures which will determine the system's order to further understand evolutionary processes in feedback substitution schemes encountered in biology. It is also possible to contrast the robustness criteria embodied in this work with other nominal perturbed feedback substitution schemes using Vinnicombe's metric. Such process would allow us to compare different feedback loops relating to biological processes that have evolved through different selection pressures.

REFERENCES

[1] J. F. Clare and D. R. White. Response time and noise power gain of electrical substitution radiometers with feedback control. *Applied Optics.* 1989, Vol. 28, 15, pp. 3417 - 3428.

[2] G. P. Liu, J. B. Yang and J. F. Whidborne, "Multiobjective Optimisation and Control", Research Studies Press LTD., 2003.

[3] H. H. Rosenbrock, "Anautomatic method for finding the greatest or least value of a function, Comp. J., 1960, 3:175-184.

[4] J. A. Nelder and R. Mead, "A simplex method for function minimization", Comp. J. , 7(4):308-313, 1965.

[5] C. M. Fonseca and P. J. Fleming, "Multiobjective optimal controller design with genetic algorithms", In Proc. Control 94, Coventry, England,1994, pp.745-749

[6] Duncan McFarlane and Keith Glover, "A Loop Shaping Procedure Using H_∞ Synthesis", IEEE Transactions on Automatic Control , vol. 37 No.6, June 1992, pp. 759- 769

[7] J. F. Whidborne, I. Postlethwaite and D.-W. Gu, "Robust Controller Design Using H_∞ Loop-Shaping and the Method of Inequalities", IEEE Trans. Control Systems Technol., Vol. 2, No. 4 December 1994

[8] C.P. Pickup, "Optimisation of the response time of averaging filters", J. Phys. E: Sci. Instrum., Vol. 14,1981, pp. 602 - 604

[9] James HM, Nichols NB and Phillips RS 1947 "Theory of Servomechanisms", Radiation Laboratory Series Vol. 25 (New York: McGraw-Hill).

[10] Andrew Chipperfield and Peter Fleming, "Multiobjective Gas Turbine Engine Controller Design Using Genetic Algorithms", IEEE Trans. Industrial Electron., Vol. 43, No. 5, 1996, pp. 583-587

[11] N. V. Dakev, J. F. Whidborne and A. J. Chipperfield, "H_∞ Design of an EMS Control System for a Maglev Vehicle Using Evolutionary Algorithms", Genetic Algorithms in Engineering Systems: Innovations and Applications, IEE, 1995, pp. 226-231

[12] K. S. Tang, K.F.Man and D.-W. Gu, "Structured Genetic Algorithm for Robust H$^\infty$ Control Systems Design", IEEE Trans. Industrial Electron., Vol. 43, No. 5, October 1996, pp.575-582.